Figure S1, Rayne *et al.*

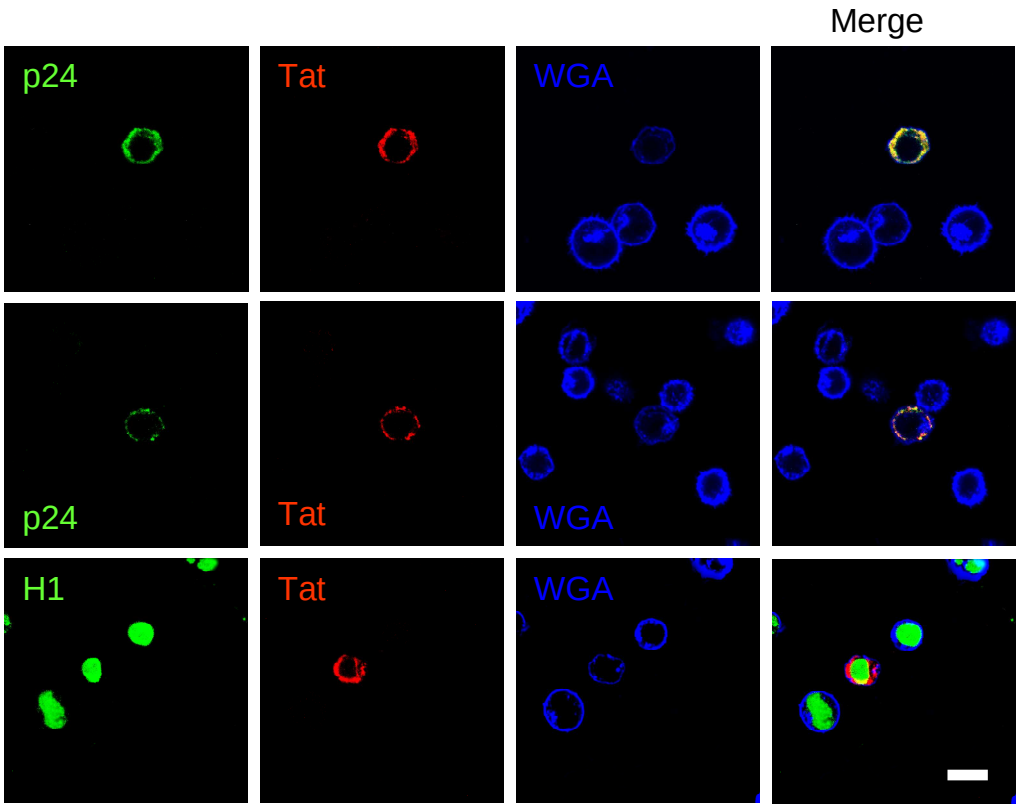

Figure S1. Widefield views of infected cells. CD4+ primary T-cells were infected with HIV-1 (pNL4-3) before processing for immunofluorescence. To this end, cells were allowed to adhere to alcian blue-treated coverslips before fixation with paraformaldehyde and permeabilization with saponin. Tat, Gag p24, or histone H1 were then revealed by immunofluorescence as indicated, while WGA was used to localize the plasma membrane and the *trans*-Golgi network. Images are medial representative confocal sections. Infected cells were weakly stained by WGA. Bar, 10 µm.

Figure S2, Rayne *et al.*

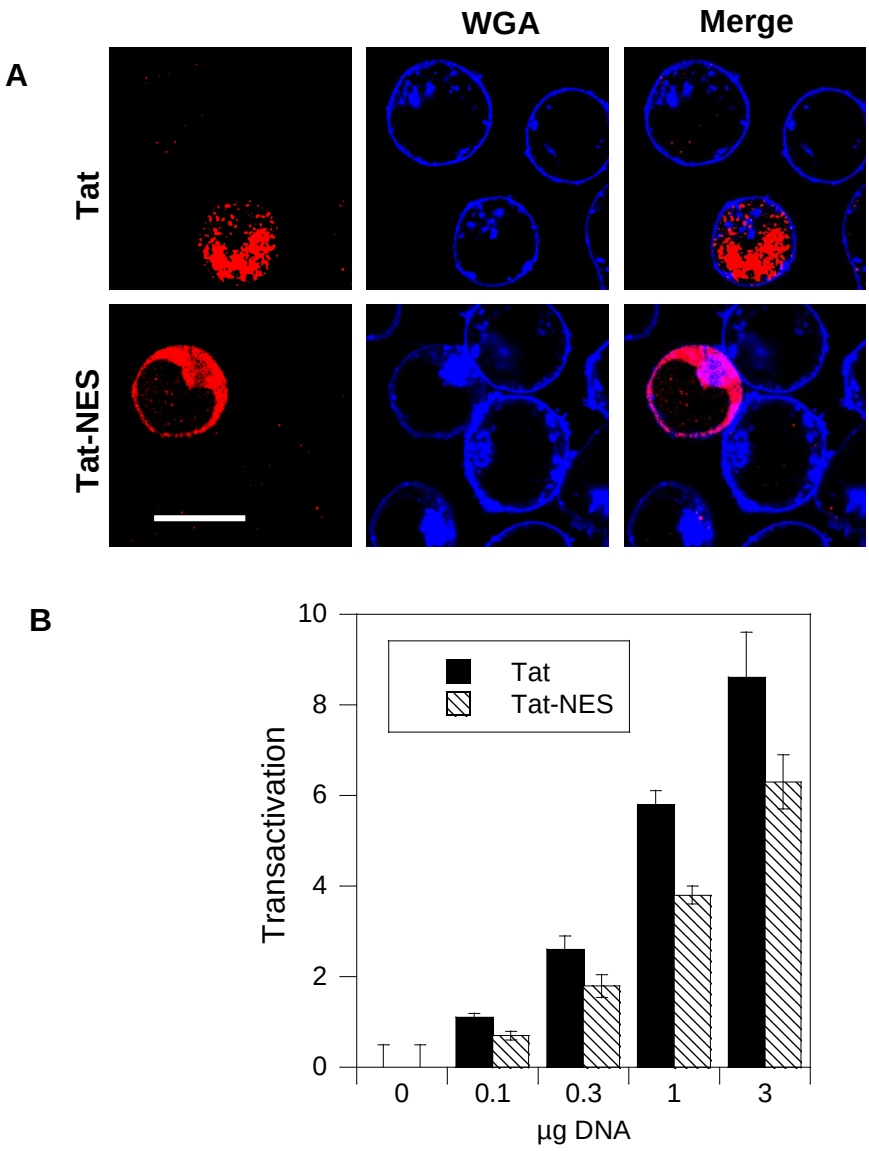

Figure S2. Tat nuclear accumulation is not required for efficient transactivation. A, Tat-NES is excluded from the nucleus. Rev nuclear export signal was attached to Tat C-terminus to obtain a Tat-NES vector that was transiently transfected into Jurkat cells. Cells were fixed and stained for Tat and WGA before observation by confocal microscopy. Median optical sections; bar, 10 µm. Tat concentrated within the nucleus while, as shown earlier in HeLa cells (Stauber, R.H. and Pavlakis, G.N. (1998) Intracellular trafficking and interactions of the HIV-1 Tat protein. *Virology*, **252**, 126-136.), Tat-NES was excluded from the nucleus and was exclusively observed in WGA-positive compartments, *i.e.* in the cytoplasm or at the plasma membrane. B, Efficiency of transactivation by Tat and Tat-NES. Jurkat cells were transfected with a fixed amount of luciferase reporter plasmids and the indicated amount of Tat- or Tat-NES vector. Transactivation by Tat-NES was ~70% that of native Tat and this ratio remained constant whatever the plasmid doses, even for low Tat/LTR ratios.

Figure S3, Rayne *et al*.

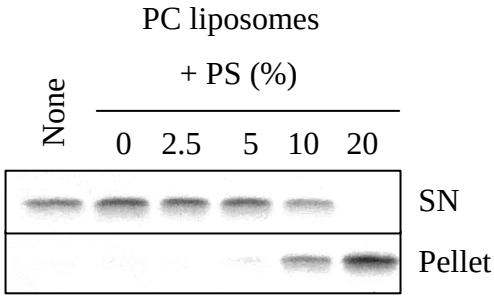

Figure S3. Effect of PS concentration on Tat binding to liposomes. Multilamellar PC liposomes containing the indicated amount of PS were incubated with Tat for 1 h at RT before ultracentrifugation. The pellet and supernatant (SN) were analyzed by SDS-PAGE for the presence of Tat. Gels were stained with Coomassie blue.

Figure S4, Rayne *et al*.

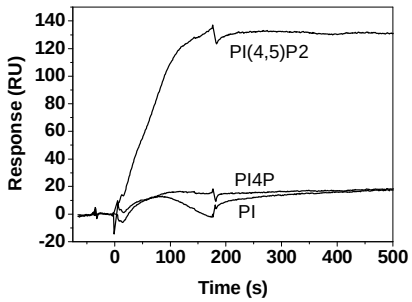

Figure S4. SPR sensorgram showing the binding of Tat (400 nM) to liposomes containing PC (75%), PE (20%) and 5% of either PI, PI4P or PI(4,5)P_2.

Figure S5, Rayne *et al*.

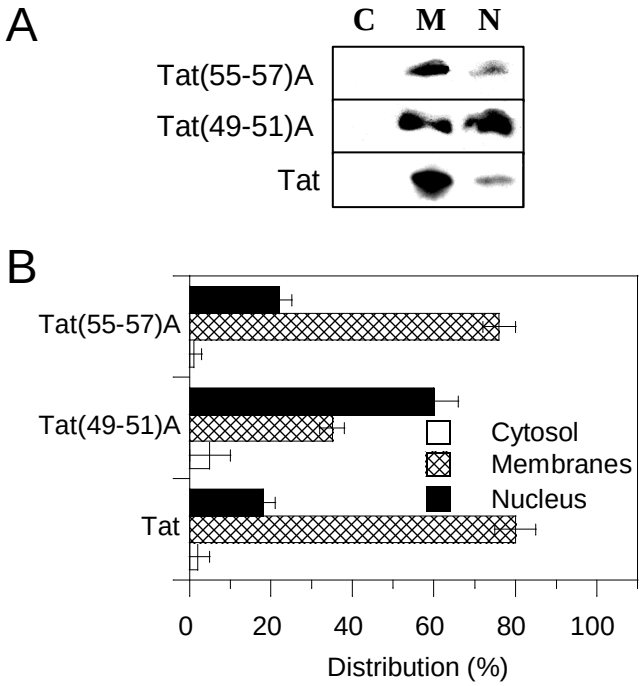

Figure S5. Disruption of Tat PIP_2-binding site results in Tat displacement from the membrane fraction. Primary $CD4^+$ T-cells were transfected with Tat-WT, Tat (49-51)A or Tat(55-57)A. One day later, cells were fractionated in three fractions, cytosolic (C), membranes (M) and nucleus (N). Proteins were precipitated and separated by Tricine SDS-PAGE before anti-Tat Western blots revealed with ECL^+ (A). The experiment was repeated three times and films were scanned for quantification using ImageQuant (B). Results are mean $\pm$ SEM (n=3).

Figure S6, Rayne *et al.*

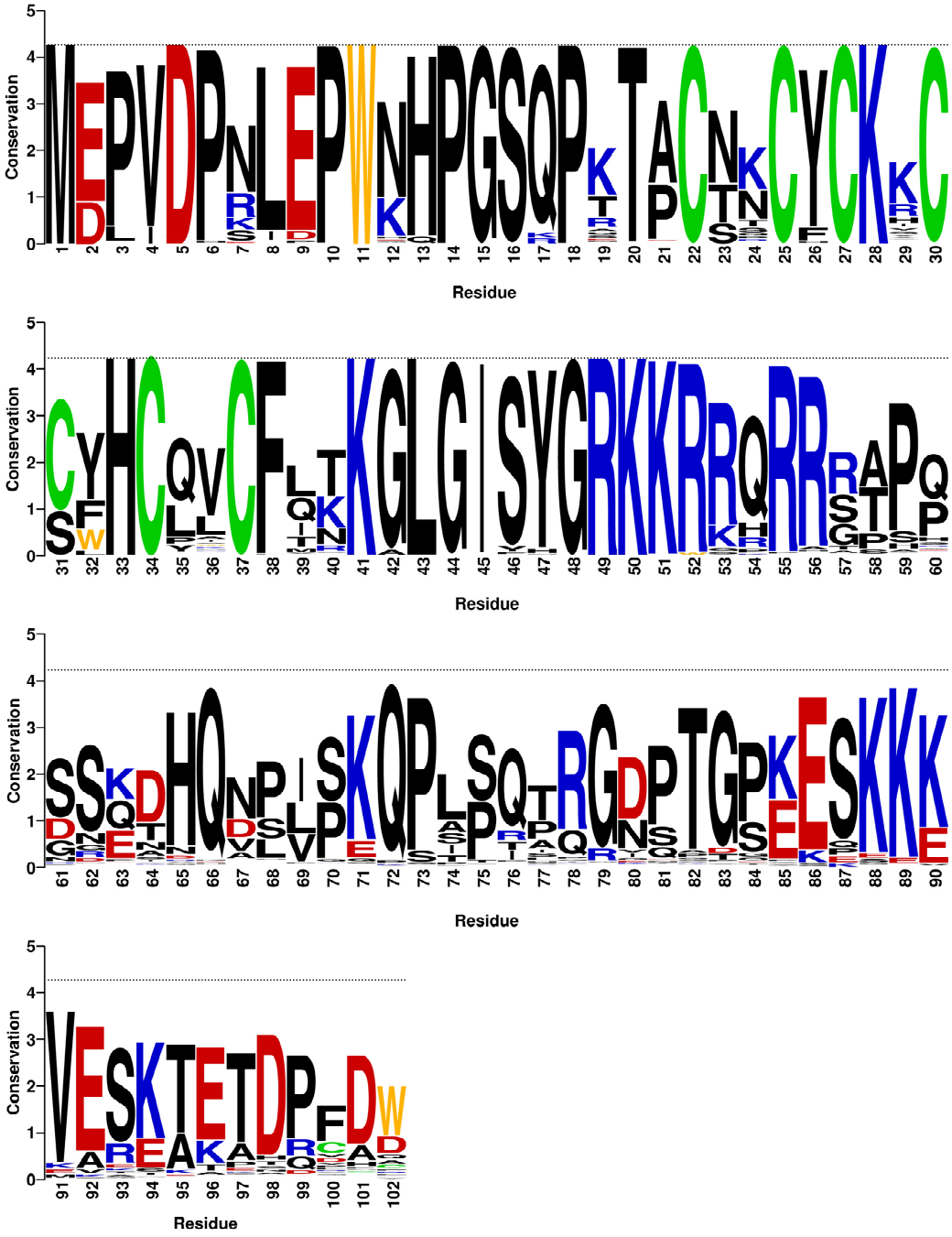

Figure S6. Tat protein sequence conservation. 1043 HIV-1 Tat sequences from Los Alamos National Laboratory database (http://www.hiv.lanl.gov/content/sequence/HIV/mainpage.html) were aligned and compared (after elimination of the gaps) using WebLogo (http://weblogo.berkeley.edu/logo.cgi). Letter size is proportional to residue conservation, and the dotted line corresponds to the conservation level of the most preserved residues. Similar data were obtained using HIV-1 Tat consensus sequence (Pantano, S. and Carloni, P. (2005) Comparative analysis of HIV-1 Tat variants. *Proteins*, **58**, 638-643.)